

Prefill-Guided Thinking for zero-shot detection of AI-generated images

Zoher Kachwala* **Danishjeet Singh** **Danielle Yang** **Filippo Menczer**
 Observatory on Social Media
 Indiana University, Bloomington, USA

Abstract

Traditional supervised methods for detecting AI-generated images depend on large, curated datasets for training and fail to generalize to novel, out-of-domain image generators. As an alternative, we explore pre-trained Vision-Language Models (VLMs) for zero-shot detection of AI-generated images. We evaluate VLM performance on three diverse benchmarks encompassing synthetic images of human faces, objects, and animals produced by 16 different state-of-the-art image generators. While off-the-shelf VLMs perform poorly on these datasets, we find that prefilling responses effectively guides their reasoning — a method we call Prefill-Guided Thinking (**PGT**). In particular, prefilling a VLM response with the phrase “*Let’s examine the style and the synthesis artifacts*” improves the Macro F1 scores of three widely used open-source VLMs by up to 24%. We analyze this improvement in detection by tracking answer confidence during response generation. For some models, pre-fills counteract early overconfidence — akin to mitigating the Dunning-Kruger effect — leading to better detection performance.

*Corresponding author: zkachwala@iu.edu

1 Introduction

Rapid advancements in image generation have led to a surge in synthetic images (deepfakes) (Goodfellow et al., 2014; Ho et al., 2020; Rombach et al., 2022). Improved techniques now enable the easier and cheaper production of high-quality visuals (Rombach et al., 2022; Li et al., 2023; Dhariwal and Nichol, 2021). These techniques benefit creative applications but also enable malicious actors to produce convincing forgeries (e.g., face swaps, synthetic photos) that are nearly indistinguishable from real ones (Li et al., 2020; Lugmayr et al., 2022; Lu et al., 2023). Such forgeries facilitate impersonation, copyright infringement, and disinformation, highlighting the urgent need for robust detection methods to maintain visual trust (Yang et al., 2024; Somepalli et al., 2023; DiResta and Goldstein, 2024; Chandra, 2024).

Existing solutions remain limited. Watermarking and metadata approaches are often easily bypassed and require widespread adoption (Zhao et al., 2024). Supervised methods, particularly feature-based ones, struggle to generalize to new generators (Li et al., 2024).

To keep pace with these rapid developments, we

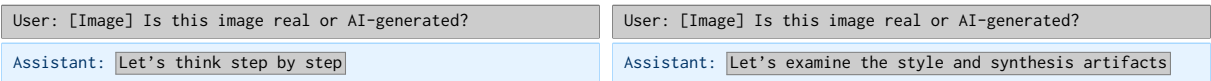


Figure 1: Top: Sample images from D3 (top row), DF40 (middle row), and GenImage (bottom row). Can you identify the real ones? (Answer in footnote.) Bottom: Guiding model responses via prefilling: chain-of-thought (left) vs task-aligned (right).

investigate the use of pre-trained Vision-Language Models (VLMs), which have demonstrated strong generalization across diverse tasks (Radford et al., 2021; Li et al., 2022, 2023) and whose performance can be further enhanced through prompting (Yang et al., 2023; Du et al., 2024).

We find that off-the-shelf VLMs perform poorly on the zero-shot detection of AI-generated images. However, prefilling a model response can guide more focused reasoning and significantly improve detection without any fine-tuning. We call this approach Prefill-Guided Thinking (**PGT**). In particular, prefilling with “*Let’s examine the style and the synthesis artifacts*” directs the VLM toward forensic cues.

We evaluate **PGT** on three diverse datasets spanning human faces, objects, and animals. These images have been generated by 16 state-of-the-art image models that produce photorealistic outputs lacking visible synthesis artifacts (Fig. 1¹). Despite this, our approach boosts Macro F1 scores by up to 24% across three open-source VLMs, generalizing across image categories and modern generators.

We explore why prefilling helps by tracking answer confidence and Macro F1 as responses progress. Baseline queries trigger immediate high confidence despite poor detection — the model commits to an answer before examining the image. For Qwen and LLaVA on most datasets, prefills counteract this overconfidence more effectively than prompts, inducing uncertainty that leads to gradually improving performance as the model’s response progresses.

2 Background

Supervised detection methods for AI-generated images typically fall into three categories: artifact-based, frequency-domain, and spatial-domain approaches.

Artifact-based methods use Convolutional Neural Networks (CNNs) or Vision Transformers (ViTs) to detect subtle cues such as unnatural textures or edge inconsistencies (Afchar et al., 2018; Rössler et al., 2019; Chollet, 2017). As generative models produce more realistic outputs, texture and edge artifacts become harder to detect. Models trained on fixed artifacts often overfit to specific generators, leading to poor generalization (Wang

et al., 2020; Cozzolino et al., 2024; Ojha et al., 2023).

Frequency-domain techniques analyze spectral representations using techniques like Fast Fourier Transform or Discrete Cosine Transform (Li et al., 2024; Dzanic et al., 2020; Frank et al., 2020; Tan et al., 2024b). These methods detected early Generative Adversarial Networks (GANs) effectively, but diffusion models produce frequency patterns that fixed-frequency detectors miss (Cozzolino et al., 2024; Baraldi et al., 2024; Zheng et al., 2024).

Spatial-domain approaches examine raw pixel patterns to detect structural or textural inconsistencies (Zheng et al., 2024; Zhou et al., 2018). While useful for earlier synthetic images, they often fail on photorealistic outputs from diffusion models and are sensitive to post-processing such as compression and resizing (Rössler et al., 2019; Bammeijer, 2024).

To improve generalization, recent work uses larger and more diverse training datasets (Wang et al., 2020; Yan et al., 2023; Ye et al., 2024; Zhu et al., 2023; Yan et al., 2024; Zhang et al., 2023; Shao et al., 2023), as well as architectural modifications that target universal artifacts (e.g., up-sampling patterns) (Zheng et al., 2024; Tan et al., 2024a). Approaches like fixed-feature backbones and DiffusionFake have also improved robustness to novel generators (Ojha et al., 2023; Sun et al., 2024).

Vision-Language Models (VLMs) are trained on large-scale image-text datasets and demonstrate strong zero-shot generalization across tasks such as classification, captioning, and visual question answering (Li et al., 2023; Radford et al., 2021; Li et al., 2022). Prompt-based learning has emerged as a lightweight method to adapt language models using natural language instructions (Brown et al., 2020). Chain-of-thought, which encourages step-by-step reasoning, has been effective in multimodal settings (Wei et al., 2022; Kojima et al., 2022; Gu et al., 2023).

Given the success of chain-of-thought prompting, we investigate whether prefilling VLM responses can enable zero-shot detection of AI-generated images. If successful, this would avoid the need for generator-specific training data.

¹Images 3, 10, and 11 are the only real ones in Fig. 1.



a) User: [Image] Is this image real or AI-generated?
 Assistant: The image appears to be real. The details, such as the texture of the strawberry's surface... (continues)
 Final Answer(real/ai-generated): real. ✗

b) User: [Image] Is this image real or AI-generated?
 Assistant: Let's think step by step
 1. Texture and Detail: The strawberry appears to have a very realistic texture... (continues)
 Final Answer(real/ai-generated): real. ✗

c) User: [Image] Is this image real or AI-generated?
 Assistant: Let's examine the style and the synthesis artifacts
 1. Texture and Detail: The strawberry appears to have a very smooth and uniform texture... (continues)
 Final Answer(real/ai-generated): ai-generated. ✓

Figure 2: PGT applied to a Midjourney-generated image of a strawberry, using Qwen2.5-7B as the VLM. Input text in `grey`; model responses in `blue`. (a) A direct query produces the incorrect answer `real`. (b) The chain-of-thought prefill `Let's think step by step` elicits step-by-step analysis, but the classification remains incorrect. (c) Our **S2** prefill `Let's examine the style and the synthesis artifacts` yields the correct classification: `ai-generated`. Full reasoning traces appear in the Appendix.

3 Methods

We frame the detection of AI-generated images as a binary classification task: given an image, the goal is to determine whether it is *real* or *AI-generated*. To evaluate overall performance, we use the Macro F1 score, which is robust to class imbalance. To analyze performance across different generators, we additionally report per-generator recall within the *AI-generated* class.

Prefill-Guided Thinking. Vision-Language Models typically consist of a *system* field for general instructions, a *user* field for inputs, and an *assistant* field for model-generated responses. A *prefill* is a phrase inserted into the *assistant* field, intended to guide the model’s response.

In our experiment, an image is presented to a VLM along with a question in the user field: `User: [Image] Is this image real or AI-generated?`. The VLM generates free-form reasoning in the assistant field (e.g., `Assistant: This image appears to be...`) (Fig. 2a). To obtain a clean label, we query the model a second time by inserting a phrase into the assistant field after its first response: `Final Answer(real/ai-generated):`. This constrains the model to select between the two labels presented in the prompt. We extract predictions using keyword matching for *real* and *ai-generated* (or its synonyms: *artificial*, *fake*, *generated*), defaulting to *real* when both appear. This is our *baseline* method.

The chain-of-thought (*CoT*) variant encour-

ages step-by-step reasoning. It uses the same initial question in the user field and inserts the phrase “*Let’s think step by step*” into the assistant field (Kojima et al., 2022). The model’s pre-filled responses then start with: `Assistant: Let's think step by step` (Fig. 2b). The final clean label is again elicited using the same follow-up answer phrase in the assistant field.

Building on prior work that highlights the importance of synthesis artifacts in detection (Jia et al., 2024), we introduce **S2**, a task-aligned prefill. We insert the phrase “*Let’s examine the style and the synthesis artifacts*” into the assistant’s field (Fig. 2c), creating a pre-filled response that starts with:

`Assistant: Let's examine the style and the synthesis artifacts`. This framing directs the model toward perceptual cues — stylistic inconsistencies or generation artifacts — rather than semantic features. The final classification label is obtained in the same way as in the baseline.

We also evaluate prefill variations and compare inserting phrases into the user field (prompting) or system field.

Data. We conduct experiments using three diverse benchmarks spanning multiple visual domains and 16 state-of-the-art image generators. Together, these datasets encompass human faces, natural objects, animals, urban scenes, artwork, and abstract imagery, with synthetic images produced by both GAN and diffusion-based architectures.

D3 is a benchmark dataset introduced as part of the Contrastive Deepfake Embeddings framework (Baraldi et al., 2024). Unlike many generative datasets focused on faces or curated categories, *D3* comprises real images collected from the web, covering a wide range of domains, including objects, urban scenes, artwork, animals, abstract visuals, and human figures. Synthetic counterparts were generated using four models: DeepFloyd IF, Stable Diffusion v1.4 and v2.1 (Rombach et al., 2022), and Stable Diffusion XL (Podell et al., 2023). We randomly sampled 2,000 sets of five images (one real and four generated). After filtering for copyright restrictions and broken links, the final dataset contains 8,420 images (1,684 real and 6,736 generated). We use 80% of this data (1,344 real and 5,392 generated) for our main evaluation and reserve the remaining 20% (344 real and 1,344 generated) for additional experiments. We refer to the main evaluation set as *D3*, and the smaller subset as *D3* (2k).

DF40 is a facial image dataset containing content generated by 40 deepfake techniques across four categories: face swapping, face reenactment, full-face synthesis, and facial editing (Yan et al., 2024). It includes outputs from state-of-the-art models such as Collaborative Diffusion (Huang et al., 2023), Midjourney, StyleCLIP (Patashnik et al., 2021), StarGAN v1 and v2 (Choi et al., 2018, 2020), and WhichFaceIsReal. The dataset spans variations in age, gender, ethnicity, and facial pose. We randomly sample 10,000 images (3,929 real and 6,071 generated) for the main evaluation, and an additional 2,000 images (794 real and 1,206 generated) for extended experiments. We refer to the main evaluation set as *DF40*, and the smaller subset as *DF40* (2k).

GenImage is built using all real images from ImageNet (Deng et al., 2009), covering diverse object categories such as animals, tools, vehicles, and furniture. Each real image is paired with a synthetic counterpart generated by one of eight models: ADM (Dhariwal and Nichol, 2021), BigGAN (Brock et al., 2018), GLIDE (Nichol et al., 2022), Midjourney, VQDM (Gu et al., 2022), Stable Diffusion v1.4 and v1.5 (Rombach et al., 2022), and Wukong. We use a balanced evaluation sample of 10,000 images (5,000 real and 5,000 generated) for the main experiments and 2,000 images (1,000 real and 1,000 generated) for extended analyses. We refer to the main evaluation set as *GenImage*, and the smaller subset as *Gen-*

Image (2k).

Collectively, our evaluation spans 28,420 images across diverse visual content and 16 generators. Modern diffusion models in these benchmarks — Stable Diffusion XL, GLIDE, Midjourney — produce photorealistic images that lack traditional synthesis artifacts (Fig. 1).

Models. We conduct experiments with three Vision-Language Models: *LLaVA-OneVision*², *Qwen2.5-VL*³, and *Llama-3.2-Vision*⁴. We use instruction-tuned variants in evaluation mode and use `seed=0` in the vLLM package (Kwon et al., 2023) to ensure reproducibility. Token generation is capped at 512 tokens (`max_tokens=512`) with `temperature=0.0` for deterministic outputs. A single run on a NVIDIA A100 80GB for 10,000 images takes approximately 3 hours.

LLaVA-OneVision is a multimodal instruction-following model; we use the 7B chat variant.

Qwen2.5-VL uses a dynamic-resolution Vision Transformer (Bai et al., 2025); we use the 7B-Instruct variant.

Llama-3.2-Vision pairs a vision adapter with a pre-trained Llama 3.1 language model; we use the 11B-Instruct variant.

4 Results

Detection Performance. With the exception of LLaVA on DF40, **S2** consistently outperforms *CoT* and the baseline across all three benchmarks and models (Fig. 3), achieving up to 24% relative improvement in Macro F1. Across all 16 generators, **S2** reliably boosts detection recall. The gains in recall range from 15% for DF40’s *sgan1* to 200% for *GenImage*’s *adm* compared to the next best method for Llama (Fig. 4). Similar trends hold for the other two models (Figs. 10, 11 in Appendix). Strong recall on Stable Diffusion XL, GLIDE, and Midjourney shows that **S2** detects photorealistic outputs without traditional synthesis artifacts. The task-aligned prefill consistently outperforms chain-of-thought.

Guidance Mode Comparison. We also compare prefill-guided thinking

²<https://huggingface.co/collections/llava-hf/llava-onevision-66bb1e9ce8856e210a7ed1fe>

³<https://huggingface.co/collections/Qwen/qwen25-vl-6795ffac22b334a837c0f9a5>

⁴<https://huggingface.co/collections/meta-llama/llama-32-66f448ffc8c32f949b04c8cf>

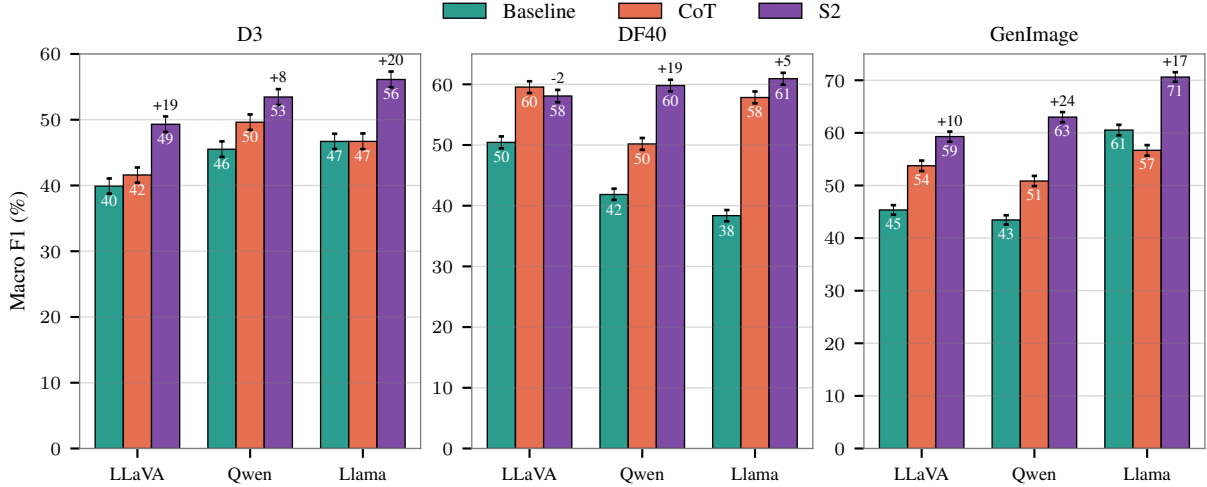


Figure 3: Detection Macro F1 across models, datasets, and **PGT** variations. Bars show relative improvement of **S2** over the next best method, with 95% confidence intervals from 10k bootstrap iterations.

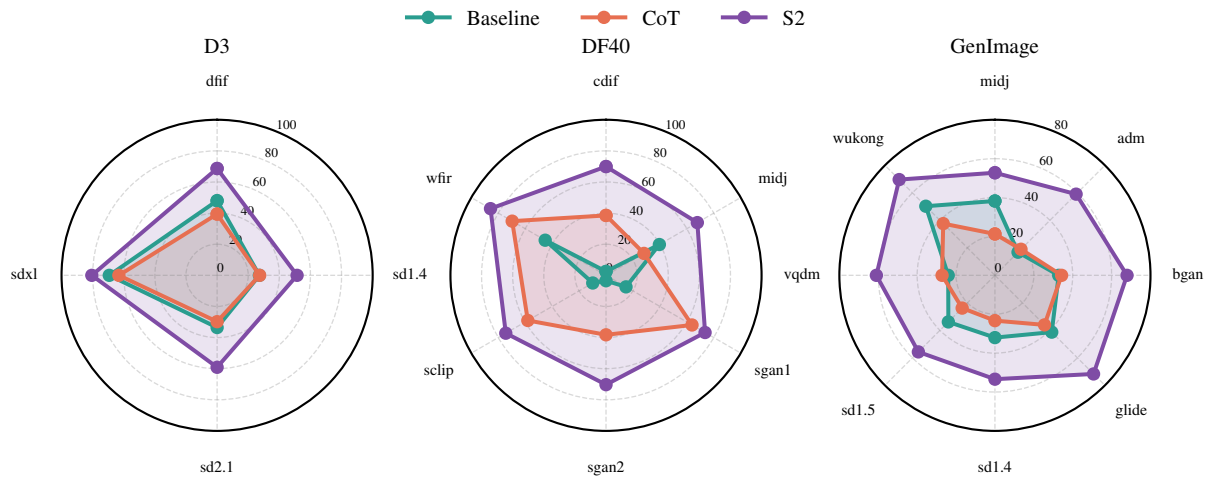


Figure 4: Detection recall (%) for Llama on each dataset, broken down by generator. Similar figures for Qwen and LLaVA are in the Appendix (Figs. 10, 11).

against simple user prompts that combine `User: [Image] Is this image real or AI-generated?` with `Please think step by step.` (*CoT*) and `Please examine the style and synthesis artifacts.` (**S2**). We also test pseudo-prefills, which use the system field to instruct the model: `System: Please start your responses with` followed by `"Let's think step by step"` or `"Let's examine the style and synthesis artifacts"`.

As shown in Table 1, user prompts and pseudo-prefills do not work as well as prefill-guided thinking for *CoT* and **S2** using Qwen. Similar trends are observed using LLaVA, whereas user prompts do work better with Llama (Tables 3, 4 in Appendix).

Prefill Phrasing. We examine sensitivity to prefill phrasing. As shown in Table 2, Qwen’s de-

tection performance varies depending on how the prefill is worded. Guiding the model to consider both style and synthesis artifacts using alternative phrasing does not reduce performance relative to our **S2** prefill. In contrast, guiding the model to focus on only style or only synthesis artifacts leads to a drop in detection. Guidance around details and flaws also proves less effective than **S2**. While phrasing affects results, any prefill guidance consistently improves performance over baseline.

5 Interpretability

To explore how different guidance modes affect model predictions, we track answer confidence and detection performance at incremental steps during response generation.

Phrase	Type	D3 (2k)	DF40 (2k)	GenImage (2k)
Baseline	—	46.7	42.3	44.5
CoT	Prefill	49.8	48.8	53.3
	Pseudo-Prefill	48.9 (-0.9)	44.1 (-4.7)	48.8 (-4.5)
	Prompt	45.5 (-4.3)	46.7 (-2.1)	50.4 (-2.9)
S2	Prefill	53.2	61.2	64.8
	Pseudo-Prefill	43.4 (-9.8)	45.2 (-16.0)	47.3 (-17.5)
	Prompt	49.7 (-3.5)	48.8 (-12.4)	50.2 (-14.6)

Table 1: Macro F1 scores (%) across datasets and guidance modes for Qwen. Values in parentheses show differences from the corresponding prefill. Tables for LLaVA and Llama are in the Appendix.

Phrase	Prefill	D3 (2k)	DF40 (2k)	GenImage (2k)
Baseline	—	46.7	42.3	44.5
CoT	Let’s think step by step	49.8	48.8	53.3
S2	Let’s examine the style and the synthesis artifacts	53.2	61.2	64.8
Variants	Let’s observe the style and the synthesis artifacts	55.6 (+2.4)	62.3 (+1.1)	64.6 (-0.2)
	Let’s examine the synthesis artifacts	54.6 (+1.4)	60.9 (-0.3)	64.0 (-0.8)
	Let’s examine the style	48.5 (-4.7)	55.7 (-5.5)	54.6 (-10.2)
	Let’s examine the details	49.2 (-4.0)	50.9 (-10.3)	51.2 (-13.6)
	Let’s examine the flaws	58.3 (+5.1)	40.0 (-21.2)	54.1 (-10.7)

Table 2: Macro F1 scores (%) of different prefill phrasings for Qwen. Variants are annotated to show absolute differences compared to S2.

Method. We conduct this analysis on the three smaller evaluation subsets — D3 (2k), DF40 (2k), GenImage (2k) — across all three models (Qwen, LLaVA, Llama) and three guidance modes (baseline, prefill, prompt). To compare confidence and performance at fixed points, we use sentence counts to divide each response into five partial-response intervals: 0%, 25%, 50%, 75%, and 100% of sentences, as illustrated in Fig. 5. For very short responses (fewer than 4 sentences), some partial responses may be empty. At each partial-response interval, we construct the input by concatenating the original query, the partial response, and the phrase `Final Answer(real/ai-generated): This image is` to elicit an answer. We generate a short completion (`temperature=0.0`, `max_tokens=20`) while tracking token-level log probabilities. Answer confidence is the mean log probability across all tokens in the generated completion. Answer predictions (real/AI-generated) are extracted using the same keyword matching approach described in Section 3.

For each data-model-guidance combination, we average answer confidence across all examples at each partial-response interval and compute Macro F1 from the pooled confusion matrix. For prompt and prefill, answer confidence and Macro F1 are further averaged across the two phrases (CoT and S2).

Results. Models guided by prefills show markedly different reasoning patterns compared to baseline and prompt methods. For baseline queries, Qwen exhibits high confidence (over 85%) from the start, which remains stable throughout its response (Fig. 6). Yet this high confidence does not translate to strong detection. Macro F1 plateaus at 42–47% after the first partial-response interval and remains flat. We interpret this as early commitment: the model selects an answer before examining the image closely, then generates reasoning that supports that choice.

Prefills reverse this pattern: Qwen’s answer confidence drops sharply at 25%, remains low through 50–75%, then recovers at 100%. Cru-

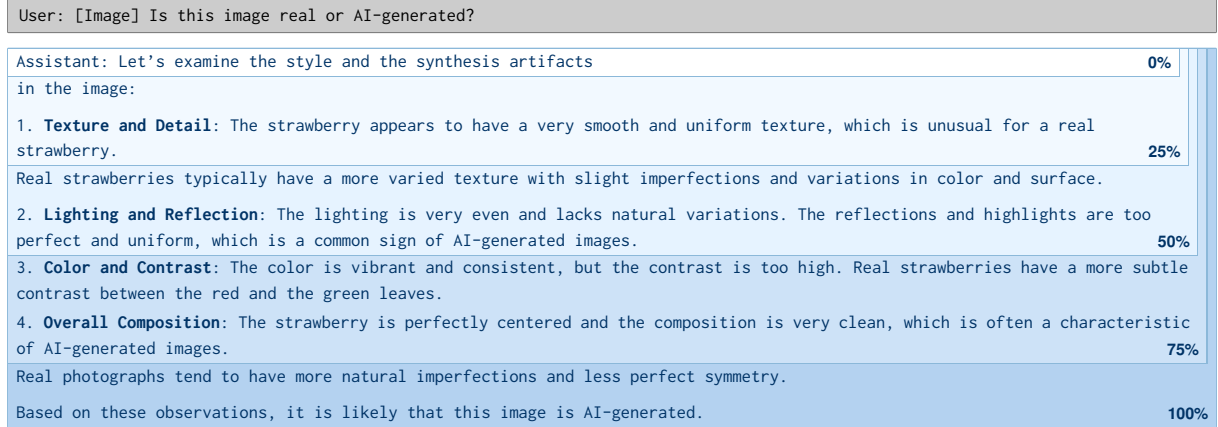


Figure 5: Example S2 prefill response at five partial-response intervals (0–100% of sentences). Nested boxes show progressively longer completions, each probed for answer confidence.

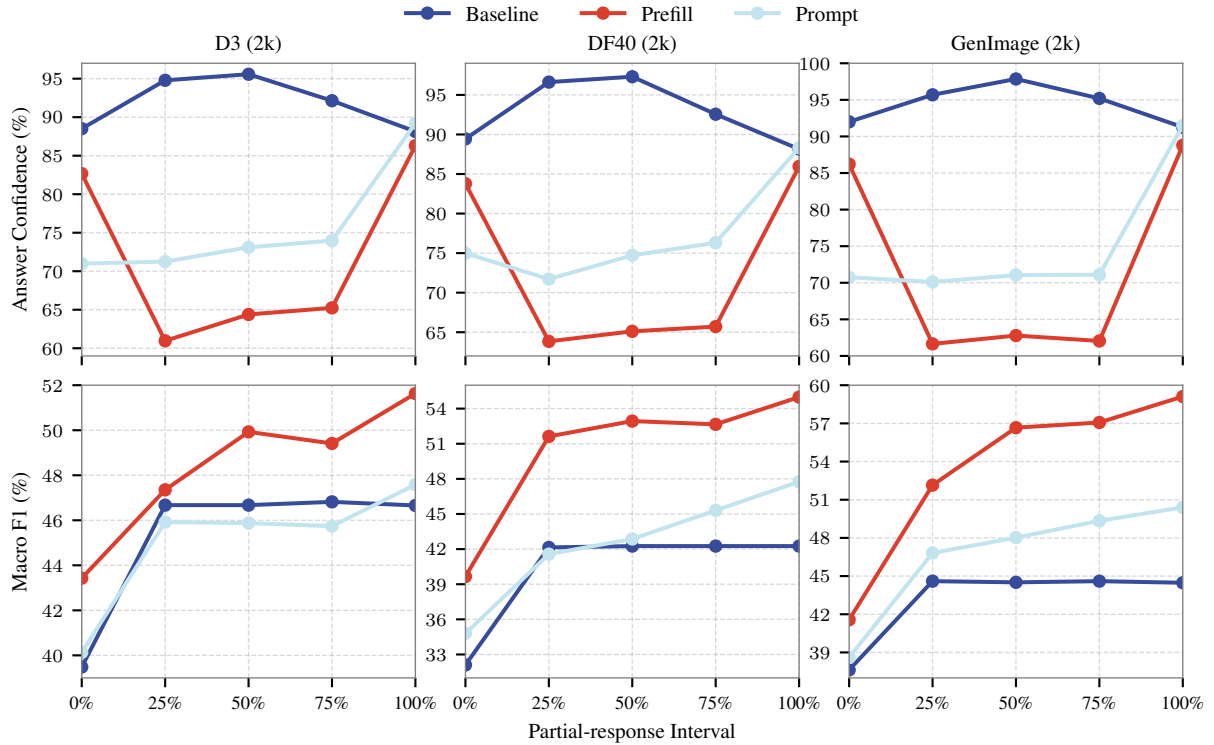


Figure 6: Evolution of answer confidence and Macro F1 across partial responses for Qwen on D3 (2k), DF40 (2k), and GenImage (2k) using baseline, prefill, and prompt guidance modes.

cially, detection performance improves steadily throughout this process. Macro F1 rises from 40–45% at the start to 52–58% at completion — the highest of any method. This confidence dip — followed by recovery only at completion — suggests that prefills delay the model’s answer selection, allowing it to accumulate image-based observations before deciding.

Prompt-guided responses maintain flat confidence throughout, with F1 gains over baseline smaller than those from prefills.

LLaVA follows similar patterns for D3 (2k) and GenImage (2k) as illustrated in Appendix Fig. 12. The exception is DF40 (2k), where prefills show no confidence dip and underperform prompts. Llama shows inconsistent patterns across datasets, with no clear relationship between confidence curves and performance (Appendix Fig. 13).

Overall, these results indicate that early overconfidence harms detection: baseline models select answers before examining the image closely,

exhibiting high confidence despite limited analysis. For some models, prefill-guided generation mitigates this effect by delaying answer selection and encouraging more deliberate reasoning.

6 Discussion

Our results show that prefilling responses for Vision-Language Models provides effective guidance for the detection of AI-generated images — without task-specific fine-tuning. We introduce a simple task-aligned prefill that consistently outperforms chain-of-thought across nearly all models and benchmarks, generalizing robustly across 16 state-of-the-art image generators — even those producing photorealistic outputs lacking traditional artifacts.

We also find that responses must be prefilled directly, as instructing the model to begin its responses with the prefill does not reliably replicate the effect. For two of the three models we tested, prefilling responses also outperforms standard user prompts. As with prompts, careful phrasing is critical for effectiveness.

What might explain these improvements? For Qwen and LLaVA on most datasets, prefills appear to counteract early overconfidence that otherwise leads to premature answers. While baseline queries trigger immediate high confidence with poor performance, prefills induce uncertainty that persists throughout the model’s response generation. This delayed commitment leads to gradually improving detection performance — suggesting that prefills may force more deliberate reasoning.

7 Limitations

A primary limitation of using VLMs for synthetic image detection is their computational cost. Compared to traditional models like CNNs or ViTs, Vision-Language Models require significantly more memory.

While we found that Prefill-Guided Thinking improves synthetic image detection across three VLMs, we cannot assume it will generalize to all VLMs. Architectures vary widely, as do their training regimes. These models were also mid-sized (7–11B parameters), so effectiveness at larger scales remains untested. Although we used state-of-the-art benchmarks from the past two years, the opaque nature of VLM training

means we cannot exclude that the models were exposed to some of these images during pre-training.

While we identified a prefill suited to synthetic image detection, our finding that prefills are sensitive to phrasing means that the ease of discovering effective prefills for any given task remains an open question.

Our interpretability analysis showed overconfidence mitigation for Qwen and LLaVA on most datasets. Llama, however, showed no clear relationship between confidence and performance. Understanding why prefills affect some architectures but not others requires further study.

Acknowledgments

This work was supported by the Knight Foundation and the Luddy School of Informatics, Computing, and Engineering at Indiana University. We gratefully acknowledge NVIDIA for the GPU access that made this study possible. This work also used Jetstream2 at Indiana University through allocation CIS240194 from the Advanced Cyberinfrastructure Coordination Ecosystem.

References

Darius Afchar, Vincent Nozick, Junichi Yamagishi, and Isao Echizen. 2018. [MesoNet: a Compact Facial Video Forgery Detection Network](#). In *2018 IEEE International Workshop on Information Forensics and Security (WIFS)*, pages 1–7. ISSN: 2157-4774.

Shuai Bai, Keqin Chen, Xuejing Liu, Jialin Wang, Wenbin Ge, Sibo Song, Kai Dang, Peng Wang, Shijie Wang, Jun Tang, Humen Zhong, Yuanzhi Zhu, Mingkun Yang, Zhaohai Li, Jianqiang Wan, Pengfei Wang, Wei Ding, Zheren Fu, Yiheng Xu, and 8 others. 2025. [Qwen2.5-VL Technical Report](#). *arXiv preprint*. ArXiv:2502.13923 [cs].

Quentin Bammey. 2024. [Synthbuster: Towards Detection of Diffusion Model Generated Images](#). *IEEE Open Journal of Signal Processing*, 5:1–9.

Lorenzo Baraldi, Federico Cocchi, Marcella Cornia, Lorenzo Baraldi, Alessandro Nicolosi, and Rita Cucchiara. 2024. [Contrasting Deepfakes Diffusion via Contrastive Learning and Global-Local Similarities](#). In *Computer Vision – ECCV 2024: 18th European Conference, Milan, Italy, September 29–October 4, 2024, Proceedings, Part LXIII*, pages 199–216, Berlin, Heidelberg. Springer-Verlag.

Andrew Brock, Jeff Donahue, and Karen Simonyan. 2018. [Large Scale GAN Training for High Fidelity Natural Image Synthesis](#). In *International Conference on Learning Representations*.

Tom B. Brown, Benjamin Mann, Nick Ryder, Melanie Subbiah, Jared Kaplan, Prafulla Dhariwal, Arvind Neelakantan, Pranav Shyam, Girish Sastry, Amanda Askell, Sandhini Agarwal, Ariel Herbert-Voss, Gretchen Krueger, Tom Henighan, Rewon Child, Aditya Ramesh, Daniel M. Ziegler, Jeffrey Wu, Clemens Winter, and 12 others. 2020. Language models are few-shot learners. In *Proceedings of the 34th International Conference on Neural Information Processing Systems*, NIPS '20, pages 1877–1901, Red Hook, NY, USA. Curran Associates Inc.

Bilva Chandra. 2024. *Analyzing Harms from AI-Generated Images and Safeguarding Online Authenticity*. RAND Corporation.

Yunjey Choi, Minje Choi, Munyoung Kim, Jung-Woo Ha, Sunghun Kim, and Jaegul Choo. 2018. **StarGAN: Unified Generative Adversarial Networks for Multi-domain Image-to-Image Translation**. In *2018 IEEE/CVF Conference on Computer Vision and Pattern Recognition*, pages 8789–8797, Salt Lake City, UT. IEEE.

Yunjey Choi, Youngjung Uh, Jaejun Yoo, and Jung-Woo Ha. 2020. **StarGAN v2: Diverse Image Synthesis for Multiple Domains**. In *2020 IEEE/CVF Conference on Computer Vision and Pattern Recognition (CVPR)*, pages 8185–8194. ISSN: 2575-7075.

François Chollet. 2017. **Xception: Deep Learning with Depthwise Separable Convolutions**. In *2017 IEEE Conference on Computer Vision and Pattern Recognition (CVPR)*, pages 1800–1807. ISSN: 1063-6919.

Davide Cozzolino, Giovanni Poggi, Riccardo Corvi, Matthias Nießner, and Luisa Verdoliva. 2024. **Raising the Bar of AI-generated Image Detection with CLIP**. In *2024 IEEE/CVF Conference on Computer Vision and Pattern Recognition Workshops (CVPRW)*, pages 4356–4366, Seattle, WA, USA. IEEE.

Jia Deng, Wei Dong, Richard Socher, Li-Jia Li, Kai Li, and Li Fei-Fei. 2009. **ImageNet: A large-scale hierarchical image database**. In *2009 IEEE Conference on Computer Vision and Pattern Recognition*, pages 248–255. ISSN: 1063-6919.

Prafulla Dhariwal and Alexander Nichol. 2021. **Diffusion Models Beat GANs on Image Synthesis**. In *Advances in Neural Information Processing Systems*, volume 34, pages 8780–8794. Curran Associates, Inc.

Renée DiResta and Josh A. Goldstein. 2024. **How spammers and scammers leverage AI-generated images on Facebook for audience growth**. *Harvard Kennedy School Misinformation Review*.

Yingjun Du, Wenfang Sun, and Cees G. Snoek. 2024. **IPO: Interpretable Prompt Optimization for Vision-Language Models**. *Advances in Neural Information Processing Systems*, 37:126725–126766.

Tarik Dzanic, Karan Shah, and Freddie Witherden. 2020. **Fourier Spectrum Discrepancies in Deep Network Generated Images**. In *Advances in Neural Information Processing Systems*, volume 33, pages 3022–3032. Curran Associates, Inc.

Joel Frank, Thorsten Eisenhofer, Lea Schönher, Asja Fischer, Dorothea Kolossa, and Thorsten Holz. 2020. **Leveraging Frequency Analysis for Deep Fake Image Recognition**. In *Proceedings of the 37th International Conference on Machine Learning*, pages 3247–3258. PMLR. ISSN: 2640-3498.

Ian J. Goodfellow, Jean Pouget-Abadie, Mehdi Mirza, Bing Xu, David Warde-Farley, Sherjil Ozair, Aaron Courville, and Yoshua Bengio. 2014. **Generative Adversarial Nets**. In *Advances in Neural Information Processing Systems*, volume 27. Curran Associates, Inc.

Jindong Gu, Zhen Han, Shuo Chen, Ahmad Beirami, Bailan He, Gengyuan Zhang, Ruotong Liao, Yao Qin, Volker Tresp, and Philip Torr. 2023. **A Systematic Survey of Prompt Engineering on Vision-Language Foundation Models**. *arXiv preprint*. ArXiv:2307.12980 [cs].

Shuyang Gu, Dong Chen, Jianmin Bao, Fang Wen, Bo Zhang, Dongdong Chen, Lu Yuan, and Baineng Guo. 2022. **Vector Quantized Diffusion Model for Text-to-Image Synthesis**. In *2022 IEEE/CVF Conference on Computer Vision and Pattern Recognition (CVPR)*, pages 10686–10696, New Orleans, LA, USA. IEEE.

Jonathan Ho, Ajay Jain, and Pieter Abbeel. 2020. **Denoising Diffusion Probabilistic Models**. In *Advances in Neural Information Processing Systems*, volume 33, pages 6840–6851. Curran Associates, Inc.

Ziqi Huang, Kelvin C.K. Chan, Yuming Jiang, and Zizwei Liu. 2023. **Collaborative Diffusion for Multi-Modal Face Generation and Editing**. In *2023 IEEE/CVF Conference on Computer Vision and Pattern Recognition (CVPR)*, pages 6080–6090, Vancouver, BC, Canada. IEEE.

Shan Jia, Reilin Lyu, Kangran Zhao, Yize Chen, Zhiyuan Yan, Yan Ju, Chuanbo Hu, Xin Li, Baoyuan Wu, and Siwei Lyu. 2024. **Can ChatGPT Detect DeepFakes? A Study of Using Multimodal Large Language Models for Media Forensics**. In *2024 IEEE/CVF Conference on Computer Vision and Pattern Recognition Workshops (CVPRW)*, pages 4324–4333, Seattle, WA, USA. IEEE.

Takeshi Kojima, Shixiang (Shane) Gu, Machel Reid, Yutaka Matsuo, and Yusuke Iwasawa. 2022. **Large Language Models are Zero-Shot Reasoners**. *Advances in Neural Information Processing Systems*, 35:22199–22213.

Woosuk Kwon, Zhuohan Li, Siyuan Zhuang, Ying Sheng, Lianmin Zheng, Cody Hao Yu, Joseph Gonzalez, Hao Zhang, and Ion Stoica. 2023. **Efficient**

Memory Management for Large Language Model Serving with PagedAttention. In *Proceedings of the 29th Symposium on Operating Systems Principles*, SOSP '23, pages 611–626, New York, NY, USA. Association for Computing Machinery.

Hanzhe Li, Jiaran Zhou, Yuezun Li, Baoyuan Wu, Bin Li, and Junyu Dong. 2024. **FreqBlender: Enhancing DeepFake Detection by Blending Frequency Knowledge**. *Advances in Neural Information Processing Systems*, 37:44965–44988.

Junnan Li, Dongxu Li, Silvio Savarese, and Steven Hoi. 2023. **BLIP-2: Bootstrapping Language-Image Pre-training with Frozen Image Encoders and Large Language Models**. In *Proceedings of the 40th International Conference on Machine Learning*, pages 19730–19742. PMLR. ISSN: 2640-3498.

Junnan Li, Dongxu Li, Caiming Xiong, and Steven Hoi. 2022. **BLIP: Bootstrapping Language-Image Pre-training for Unified Vision-Language Understanding and Generation**. In *Proceedings of the 39th International Conference on Machine Learning*, pages 12888–12900. PMLR. ISSN: 2640-3498.

Lingzhi Li, Jianmin Bao, Hao Yang, Dong Chen, and Fang Wen. 2020. **Advancing High Fidelity Identity Swapping for Forgery Detection**. In *2020 IEEE/CVF Conference on Computer Vision and Pattern Recognition (CVPR)*, pages 5073–5082, Seattle, WA, USA. IEEE.

Zeyu Lu, Di Huang, Lei Bai, Jingjing Qu, Chengyue Wu, Xihui Liu, and Wanli Ouyang. 2023. **Seeing is not always believing: Benchmarking Human and Model Perception of AI-Generated Images**. *Advances in Neural Information Processing Systems*, 36:25435–25447.

Andreas Lugmayr, Martin Danelljan, Andres Romero, Fisher Yu, Radu Timofte, and Luc Van Gool. 2022. **RePaint: Inpainting using Denoising Diffusion Probabilistic Models**. In *2022 IEEE/CVF Conference on Computer Vision and Pattern Recognition (CVPR)*, pages 11451–11461, New Orleans, LA, USA. IEEE.

Alexander Quinn Nichol, Prafulla Dhariwal, Aditya Ramesh, Pranav Shyam, Pamela Mishkin, Bob McGrew, Ilya Sutskever, and Mark Chen. 2022. **GLIDE: Towards Photorealistic Image Generation and Editing with Text-Guided Diffusion Models**. In *Proceedings of the 39th International Conference on Machine Learning*, pages 16784–16804. PMLR. ISSN: 2640-3498.

Utkarsh Ojha, Yuheng Li, and Yong Jae Lee. 2023. **Towards Universal Fake Image Detectors that Generalize Across Generative Models**. In *2023 IEEE/CVF Conference on Computer Vision and Pattern Recognition (CVPR)*, pages 24480–24489, Vancouver, BC, Canada. IEEE.

Or Patashnik, Zongze Wu, Eli Shechtman, Daniel Cohen-Or, and Dani Lischinski. 2021. **StyleCLIP: Text-Driven Manipulation of StyleGAN Imagery**. In *2021 IEEE/CVF International Conference on Computer Vision (ICCV)*, pages 2065–2074, Montreal, QC, Canada. IEEE.

Dustin Podell, Zion English, Kyle Lacey, Andreas Blattmann, Tim Dockhorn, Jonas Müller, Joe Penna, and Robin Rombach. 2023. **SDXL: Improving Latent Diffusion Models for High-Resolution Image Synthesis**. In *The Twelfth International Conference on Learning Representations*.

Alec Radford, Jong Wook Kim, Chris Hallacy, Aditya Ramesh, Gabriel Goh, Sandhini Agarwal, Girish Sastry, Amanda Askell, Pamela Mishkin, Jack Clark, Gretchen Krueger, and Ilya Sutskever. 2021. **Learning Transferable Visual Models From Natural Language Supervision**. In *Proceedings of the 38th International Conference on Machine Learning*, pages 8748–8763. PMLR. ISSN: 2640-3498.

Robin Rombach, Andreas Blattmann, Dominik Lorenz, Patrick Esser, and Bjorn Ommer. 2022. **High-Resolution Image Synthesis with Latent Diffusion Models**. In *2022 IEEE/CVF Conference on Computer Vision and Pattern Recognition (CVPR)*, pages 10674–10685, New Orleans, LA, USA. IEEE.

Andreas Rössler, Davide Cozzolino, Luisa Verdoliva, Christian Riess, Justus Thies, and Matthias Niessner. 2019. **FaceForensics++: Learning to Detect Manipulated Facial Images**. In *2019 IEEE/CVF International Conference on Computer Vision (ICCV)*, pages 1–11. ISSN: 2380-7504.

Rui Shao, Tianxing Wu, and Ziwei Liu. 2023. **Detecting and Grounding Multi-Modal Media Manipulation**. In *2023 IEEE/CVF Conference on Computer Vision and Pattern Recognition (CVPR)*, pages 6904–6913, Vancouver, BC, Canada. IEEE.

Gowthami Somepalli, Vasu Singla, Micah Goldblum, Jonas Geiping, and Tom Goldstein. 2023. **Diffusion Art or Digital Forgery? Investigating Data Replication in Diffusion Models**. In *2023 IEEE/CVF Conference on Computer Vision and Pattern Recognition (CVPR)*, pages 6048–6058, Vancouver, BC, Canada. IEEE.

Ke Sun, Shen Chen, Taiping Yao, Hong Liu, Xiaoshuai Sun, Shouhong Ding, and Rongrong Ji. 2024. **DiffusionFake: Enhancing Generalization in Deepfake Detection via Guided Stable Diffusion**. *Advances in Neural Information Processing Systems*, 37:101474–101497.

Chuangchuang Tan, Huan Liu, Yao Zhao, Shikui Wei, Guanghua Gu, Ping Liu, and Yunchao Wei. 2024a. **Rethinking the Up-Sampling Operations in CNN-Based Generative Network for Generalizable Deepfake Detection**. In *2024 IEEE/CVF Conference on Computer Vision and Pattern Recognition (CVPR)*, pages 28130–28139, Seattle, WA, USA. IEEE.

Chuangchuang Tan, Yao Zhao, Shikui Wei, Guanghua Gu, Ping Liu, and Yunchao Wei. 2024b. Frequency-aware deepfake detection: improving generalizability through frequency space domain learning. In *Proceedings of the Thirty-Eighth AAAI Conference on Artificial Intelligence and Thirty-Sixth Conference on Innovative Applications of Artificial Intelligence and Fourteenth Symposium on Educational Advances in Artificial Intelligence*, volume 38 of *AAAI'24/IAAI'24/EAAI'24*, pages 5052–5060. AAAI Press.

Sheng-Yu Wang, Oliver Wang, Richard Zhang, Andrew Owens, and Alexei A. Efros. 2020. CNN-Generated Images Are Surprisingly Easy to Spot... for Now. In *2020 IEEE/CVF Conference on Computer Vision and Pattern Recognition (CVPR)*, pages 8692–8701. IEEE Computer Society.

Jason Wei, Xuezhi Wang, Dale Schuurmans, Maarten Bosma, Brian Ichter, Fei Xia, Ed Chi, Quoc V. Le, and Denny Zhou. 2022. Chain-of-Thought Prompting Elicits Reasoning in Large Language Models. *Advances in Neural Information Processing Systems*, 35:24824–24837.

Zhiyuan Yan, Taiping Yao, Shen Chen, Yandan Zhao, Xinghe Fu, Junwei Zhu, Donghao Luo, Chengjie Wang, Shouhong Ding, Yunsheng Wu, and Li Yuan. 2024. DF40: Toward Next-Generation Deepfake Detection. *Advances in Neural Information Processing Systems*, 37:29387–29434.

Zhiyuan Yan, Yong Zhang, Xinhang Yuan, Siwei Lyu, and Baoyuan Wu. 2023. DeepfakeBench: A Comprehensive Benchmark of Deepfake Detection. *arXiv preprint*. ArXiv:2307.01426 [cs].

Kaicheng Yang, Danishjeet Singh, and Filippo Menczer. 2024. Characteristics and Prevalence of Fake Social Media Profiles with AI-generated Faces. *Journal of Online Trust and Safety*, 2(4). Number: 4.

Lingfeng Yang, Yueze Wang, Xiang Li, Xinlong Wang, and Jian Yang. 2023. Fine-Grained Visual Prompting. *Advances in Neural Information Processing Systems*, 36:24993–25006.

Junyan Ye, Baichuan Zhou, Zilong Huang, Junan Zhang, Tianyi Bai, Hengrui Kang, Jun He, Honglin Lin, Zihao Wang, Tong Wu, Zhizheng Wu, Yiping Chen, Dahua Lin, Conghui He, and Weijia Li. 2024. LOKI: A Comprehensive Synthetic Data Detection Benchmark using Large Multimodal Models. In *The Thirteenth International Conference on Learning Representations*.

Lingzhi Zhang, Zhengjie Xu, Connelly Barnes, Yuqian Zhou, Qing Liu, He Zhang, Sohrab Amirghodsi, Zhe Lin, Eli Shechtman, and Jianbo Shi. 2023. Perceptual Artifacts Localization for Image Synthesis Tasks. In *2023 IEEE/CVF International Conference on Computer Vision (ICCV)*, pages 7545–7556, Paris, France. IEEE.

Xuandong Zhao, Kexun Zhang, Zihao Su, Saastha Vasan, Ilya Grishchenko, Christopher Kruegel, Giovanni Vigna, Yu-Xiang Wang, and Lei Li. 2024. Invisible Image Watermarks Are Provably Removable Using Generative AI. *Advances in Neural Information Processing Systems*, 37:8643–8672.

Chende Zheng, Chenhao Lin, Zhengyu Zhao, Hang Wang, Xu Guo, Shuai Liu, and Chao Shen. 2024. Breaking Semantic Artifacts for Generalized AI-generated Image Detection. *Advances in Neural Information Processing Systems*, 37:59570–59596.

Peng Zhou, Xintong Han, Vlad I. Morariu, and Larry S. Davis. 2018. Learning Rich Features for Image Manipulation Detection. In *2018 IEEE/CVF Conference on Computer Vision and Pattern Recognition*, pages 1053–1061. ISSN: 2575-7075.

Mingjian Zhu, Hanting Chen, Qiangyu Yan, Xudong Huang, Guanyu Lin, Wei Li, Zhijun Tu, Hailin Hu, Jie Hu, and Yunhe Wang. 2023. GenImage: A Million-Scale Benchmark for Detecting AI-Generated Image. *Advances in Neural Information Processing Systems*, 36:77771–77782.

A Appendix

A.1 Full Reasoning Traces

This section includes the full reasoning traces for all three methods. We can see the full traces produced by Qwen's PGT variations for the AI-generated image of a strawberry (Figs 7, 8, 9).

User: [Image] Is this image real or AI-generated?
Assistant: The image appears to be real. The details, such as the texture of the strawberry's surface, the natural color gradient, and the lighting, are consistent with a photograph of a real strawberry. There are no visible artifacts or anomalies that would suggest it is AI-generated.
Final Answer(real/ai-generated): real. ✗

Figure 7: An example of a baseline reasoning trace for detecting AI-generated images using a VLM (Qwen2.5-7B). Image from Fig. 2.

User: [Image] Is this image real or AI-generated?
Assistant [Let's think step by step]:
1. Texture and Detail: The strawberry appears to have a very realistic texture. The surface of the strawberry, including the tiny seeds and the green leafy top, looks natural and detailed.
2. Lighting and Shadows: The lighting on the strawberry is well-balanced, with a soft shadow cast on the surface. This is typical of real-life photography where light interacts with the object in a natural way.
3. Color and Contrast: The colors are vibrant and natural. The red of the strawberry and the green of the leafy top are consistent with what you would expect from a real strawberry.
4. Overall Composition: The composition of the image is natural and unposed, which is more likely to be a real photograph rather than an AI-generated image.
Given these observations, it is likely that this image is a real photograph of a strawberry. However, it's important to note that AI-generated images can sometimes be very realistic, so it's always a good idea to use multiple detection methods.
Final Answer(real/ai-generated): real. ✗

Figure 8: An example of a chain-of-thought reasoning trace for detecting AI-generated images using a VLM (Qwen2.5-7B). Image from Fig. 2.

User: [Image] Is this image real or AI-generated?
Assistant [Let's examine the style and synthesis artifacts] in the image:
1. Texture and Detail: The strawberry appears to have a very smooth and uniform texture, which is somewhat unusual for a real strawberry. Real strawberries typically have more varied and natural texture, with slight imperfections and variations in color and surface.
2. Lighting and Reflection: The lighting on the strawberry is very even and lacks the natural variations you would expect in a real fruit. The reflections and highlights are too perfect and uniform, which is a common sign of AI-generated images.
3. Color and Contrast: The color of the strawberry is vibrant and consistent, but the contrast is too high. Real strawberries have a more subtle contrast between the red and the green leaves, and the overall color gradient is not as sharp.
4. Overall Composition: The strawberry is perfectly centered and the composition is very clean, which is often a characteristic of AI-generated images. Real photographs tend to have more natural imperfections and less perfect symmetry.
Based on these observations, it is likely that this image is AI-generated.
Final Answer(real/ai-generated): ai-generated. ✓

Figure 9: An example of a S2 reasoning trace for detecting AI-generated images using a VLM (Qwen2.5-7B). Image from Fig. 2.

A.2 Detection Recall

This section shows the detection recall for Qwen and LLaVA (Figs 10, 11).

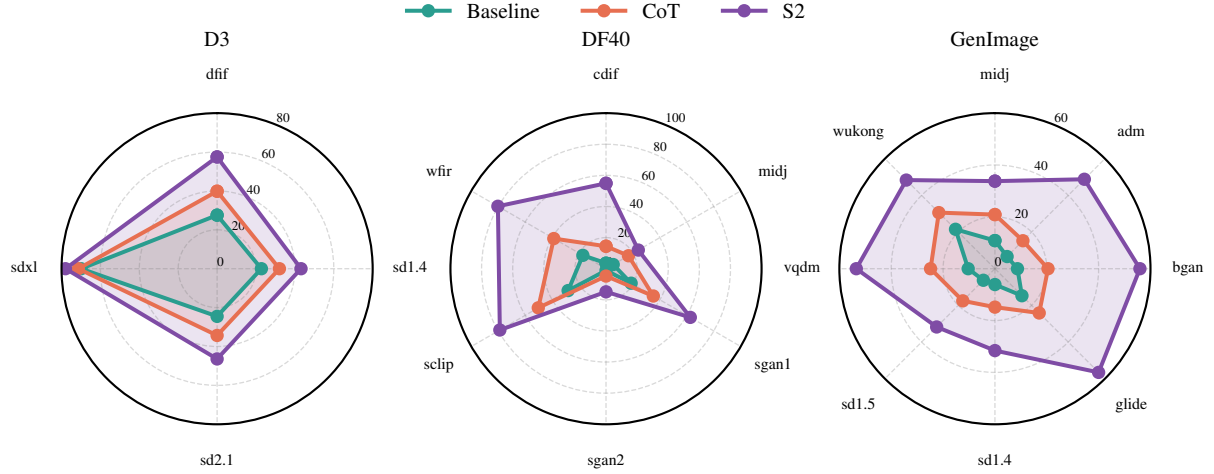


Figure 10: Detection recall (%) for Qwen on each dataset, broken down by generator.

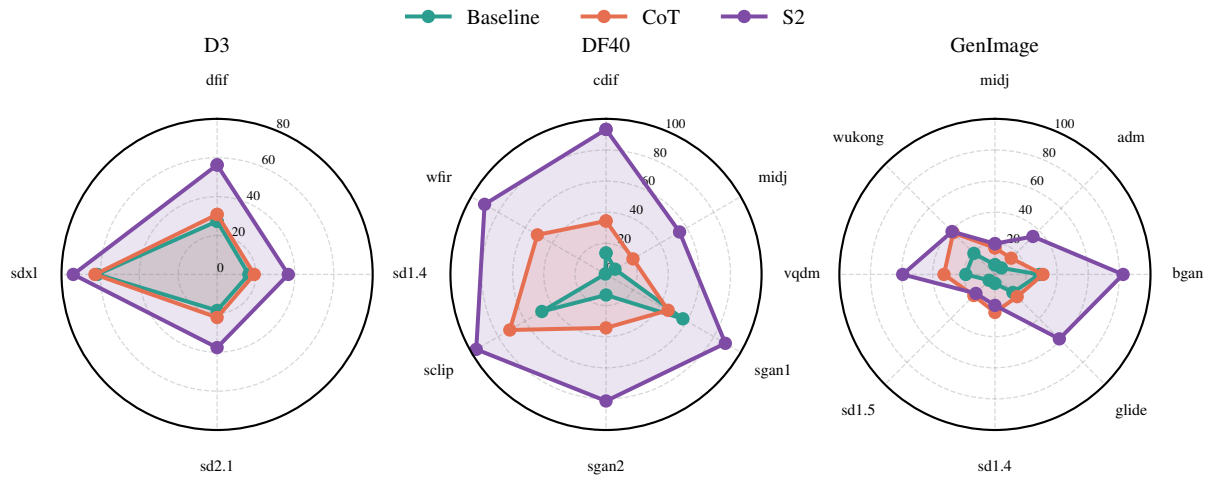


Figure 11: Detection recall (%) for LLaVA on each dataset, broken down by generator.

A.3 Guidance Comparison

This section shows the detection performance for LLaVA and Llama across guidance variations of chain-of-thought and **S2** (Tables 3, 4).

A.4 Confidence Analysis

This section expands the partial response analysis to LLaVA and Llama (Figs 12, 13).

Phrase	Type	D3 (2k)	DF40 (2k)	GenImage (2k)
Baseline	—	41.8	49.3	45.1
CoT	Prefill	44.2	59.2	55.1
	Pseudo-Prefill	41.3 (-2.9)	49.1 (-10.1)	45.6 (-9.5)
	Prompt	43.5 (-0.7)	52.2 (-7.0)	55.4 (+0.3)
S2	Prefill	52.1	57.5	59.6
	Pseudo-Prefill	41.6 (-10.5)	49.2 (-8.3)	45.6 (-14.0)
	Prompt	45.0 (-7.1)	60.6 (+3.1)	52.2 (-7.4)

Table 3: Macro F1 scores (%) across datasets and guidance modes for LLaVA. Values in parentheses show differences from the corresponding prefill.

Phrase	Type	D3 (2k)	DF40 (2k)	GenImage (2k)
Baseline	—	47.7	40.1	60.4
CoT	Prefill	47.8	60.3	58.1
	Pseudo-Prefill	40.7 (-7.1)	50.3 (-10.0)	47.4 (-10.7)
	Prompt	50.5 (+2.7)	61.5 (+1.2)	62.9 (+4.8)
S2	Prefill	58.4	62.1	71.8
	Pseudo-Prefill	58.6 (+0.2)	58.7 (-3.4)	64.4 (-7.4)
	Prompt	56.5 (-1.9)	63.1 (+1.0)	76.6 (+4.8)

Table 4: Macro F1 scores (%) across datasets and guidance modes for Llama. Values in parentheses show differences from the corresponding prefill.

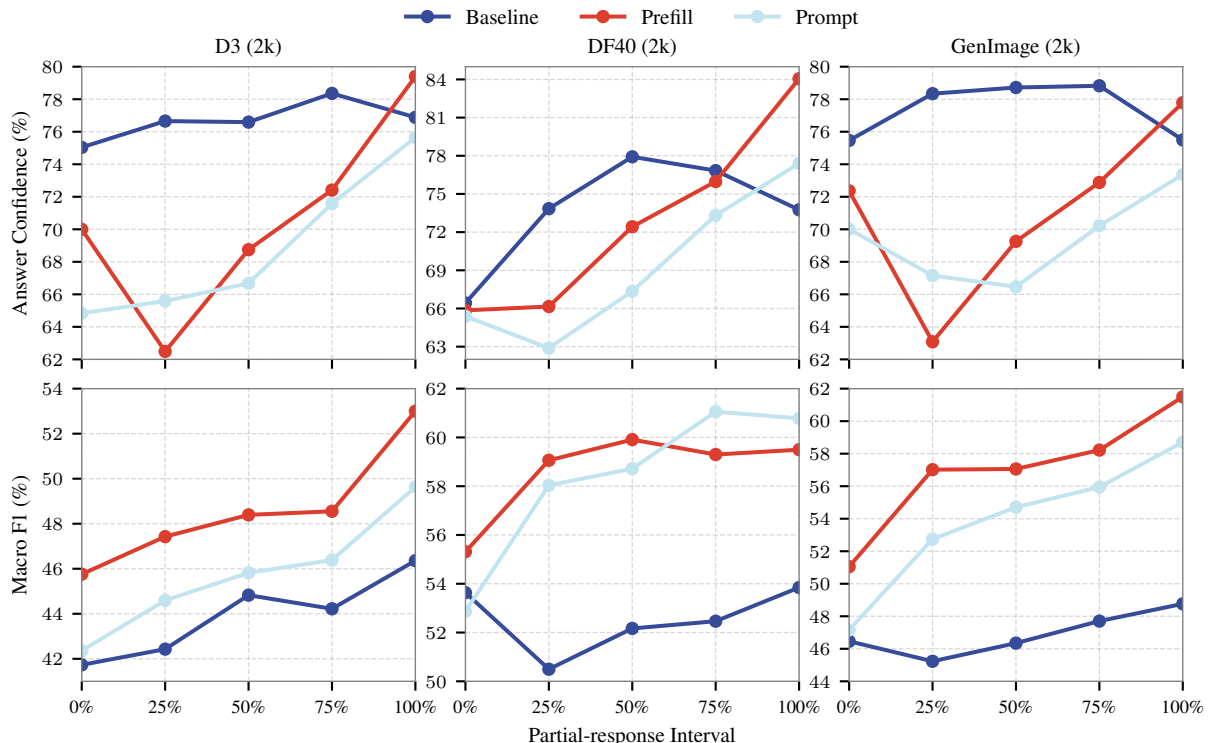


Figure 12: Evolution of answer confidence and Macro F1 across partial responses for LLaVA on D3 (2k), DF40 (2k), and GenImage (2k) using baseline, prefill, and prompt guidance modes.

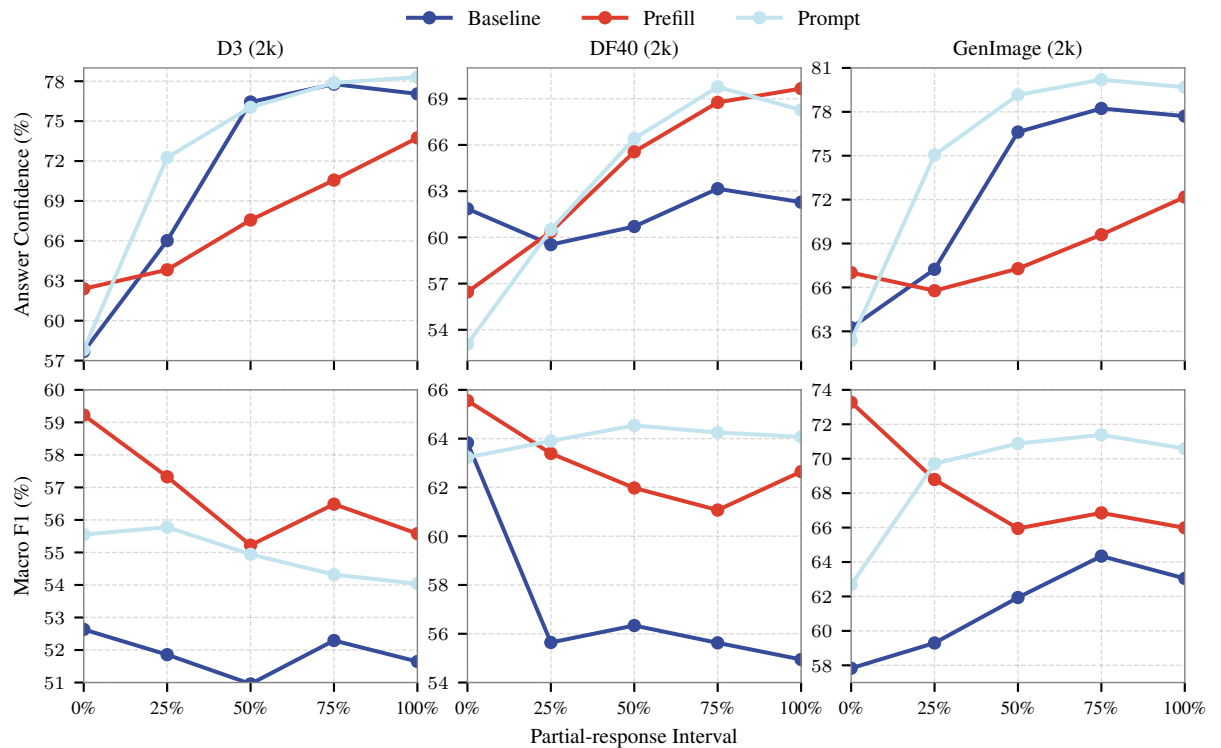


Figure 13: Evolution of answer confidence and Macro F1 across partial responses for Llama on D3 (2k), DF40 (2k), and GenImage (2k) using baseline, prefill, and prompt guidance modes.